

Preliminary Design Study of a Pre-booster Damping Ring for the FCC e^+e^- Injector

O. Etisken,¹ Y. Papaphilippou,² and A.K. Ciftci^{1,3}

¹Ankara University, Ankara, Turkey

²CERN, Geneva, Switzerland

³Izmir University of Economics, Izmir, Turkey

Abstract

The aim of the FCC e^+e^- lepton collider is to collide particles in the energy range 40–175 GeV. The FCC e^+e^- injector complex needs to produce and transport high-intensity e^+e^- beams at a fast repetition rate of about 0.1 Hz to top up the collider at its collision energy. A basic parameter set exists for all collider energies, assuming a 10 GeV linac operating with a large number of bunches accumulating in the existing SPS, which serves as pre-accelerator and damping ring before the bunches are transferred to the high-energy booster. The purpose of this study is to provide the conceptual design of an alternative damping and accelerator ring, replacing the SPS in the current scheme. This ring will have an injection energy of around 6 GeV and an extraction energy of around 20 GeV. Apart from establishing the basic ring parameters, the final study will include the optics design and layout, and single particle linear and non-linear dynamics optimization, including magnetic and alignment error tolerances. The study will also involve some basic estimation of collective effects, including intrabeam scattering, single and multibunch instabilities and impedances, two-stream effects (e-cloud and ion instabilities) and address the issue of synchrotron radiation handling. In this document, as part of these studies, basic ring parameters, first results of optical design after some analytical calculations, and layout studies are presented.

Keywords

FCC; damping ring; pre-booster ring.

1 Introduction

The current design plan considers the SPS (super proton synchrotron) as a pre-booster damping ring but there may be issues with it: machine availability, synchrotron radiation, new RF system, etc. For these reasons, a ‘green-field’ alternative design was found interesting; the study is concentrated on a new design for pre-accelerating the bunches before they are transferred to the main booster ring. First, it was planned to design a pre-booster ring design with an injection energy of 6 GeV and an extraction energy of 30 GeV. For this goal, the ring design was studied with parameter scaling and basic calculations to determine general parameters. After investigating parameter scaling of the pre-booster with 30 GeV extraction energy, our results forced us to concentrate on an extraction energy of 20 GeV for the pre-booster, since it gives a more logical perimeter for the machine [1]. Following this determination of the extraction energy as 20 GeV, a parameter scaling study and basic calculations were made and the conceptual design and straight sections were studied; in presenting these studies, phase advance, chromaticity, and emittance changes were also investigated.

2 Parameter scaling

Some important parameters, investigated to determine general parameter scaling of the machine, are:

- energy loss per turn;
- damping times;
- energy spread;
- emittance.

All these parameters are correlated with the circumference and filling factor (FF), so this gives an opportunity to compare all the parameters with each other easily:

$$FF = \frac{Nl}{C}, \quad (1)$$

where N is dipole quantity, l is dipole length, and C is circumference.

Figure 1 shows a plot of energy loss per turn for the extraction energy of 30 GeV.

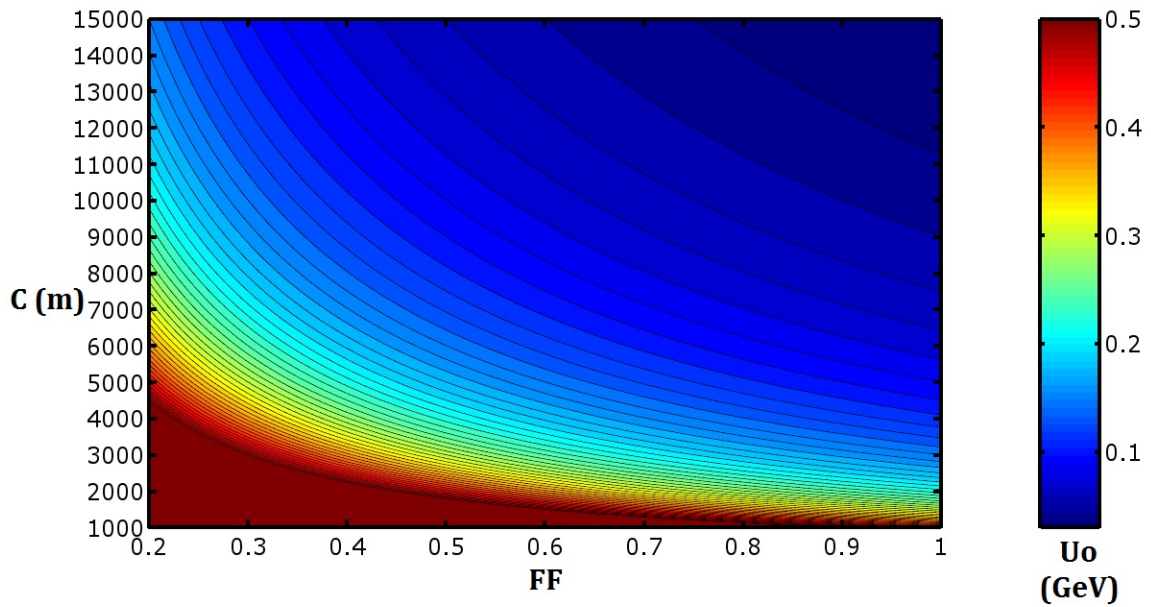


Fig. 1: Scaling of energy loss per turn with filling factor FF and circumference C for 30 GeV

Not having much more than 50 MeV energy loss per turn was one of the assumptions that we made during the study. It is shown in the graph that a circumference shorter than 10 km is not possible for the ≈ 50 MeV energy loss per turn, and having a freshly designed pre-booster 10 km long could not be logical, considering that the existing plan for the SPS is nearly 7 km long [2].

These results motivated us to study 20 GeV extraction energy. Thus, scaling of energy loss per turn was investigated for 20 GeV extraction energy, as shown in Fig. 2.

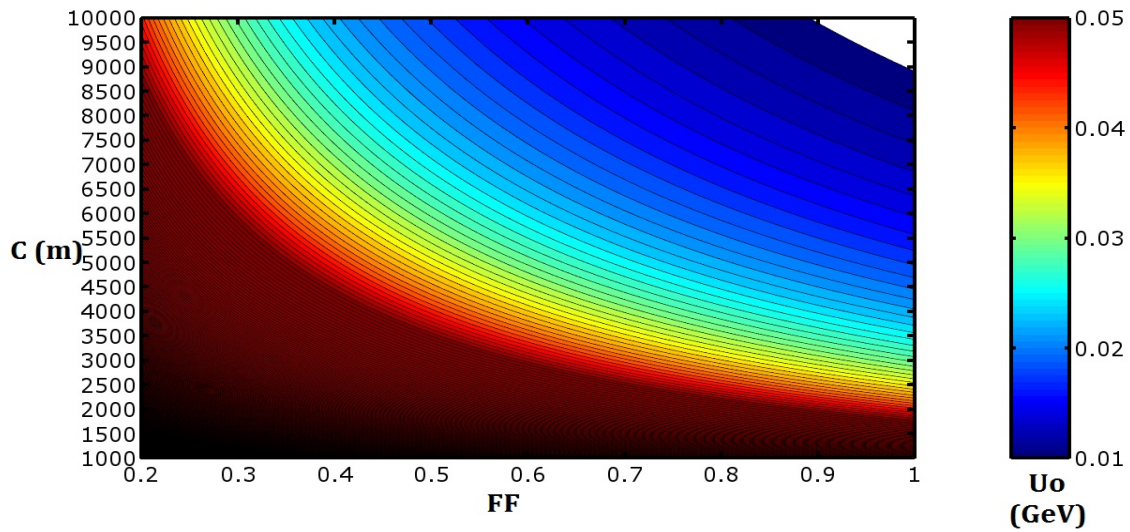


Fig. 2: Scaling of energy loss per turn with filling factor FF and circumference C for 20 GeV

From Fig. 2, it can be seen that 20 GeV enables us to have a circumference of about 2.5 km. With this good result for the machine, it became reasonable to review all other parameters, as shown in Figs. 3–5, for this energy.

As seen from Fig. 2, considering that the FF could be between 0.5 and 0.8, the circumference would have to be between 2 km and 5 km. These parameters give us the necessary frame for considering the other plots.

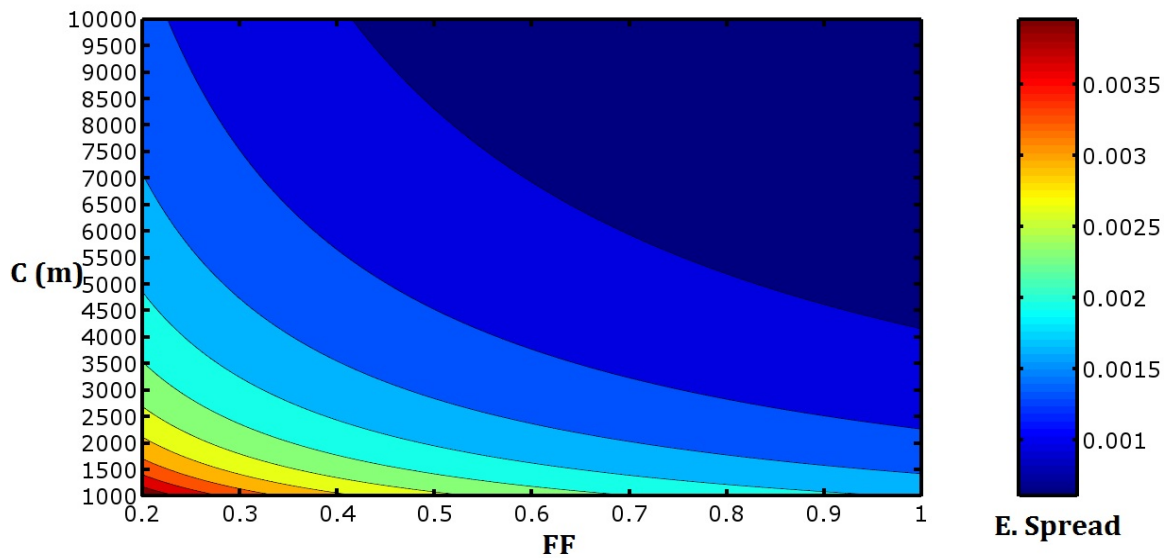


Fig. 3: Scaling of energy spread with filling factor FF and circumference C for 20 GeV

Figure 3 shows that the energy spread is acceptable and does not vary too much in the frame that was determined for our scaling. The same comments can be made for damping time, as can be seen in Fig. 4.

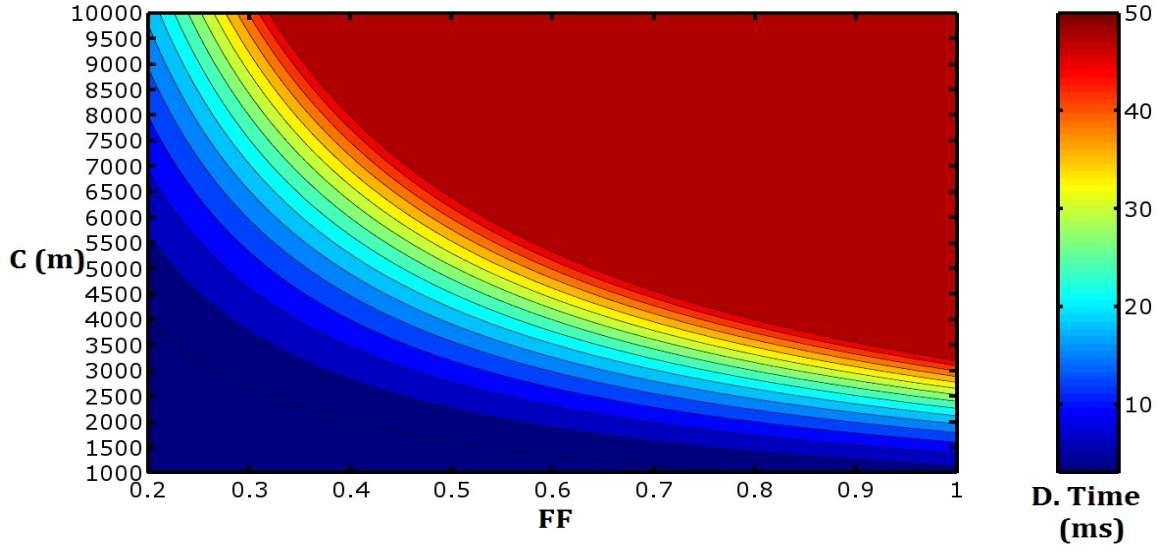


Fig. 4: Scaling of damping time with filling factor FF and circumference C for 20 GeV

After reviewing Figs. 1–4, emittance scaling could also be a good parameter to investigate for the machine:

$$\varepsilon_s = \frac{F_{\text{lattice}} \cdot C_q \cdot \gamma^2 \cdot (2\pi)^3 \cdot l^3}{FF^3 \cdot C^3}. \quad (2)$$

The result shown in Fig. 5 gives us emittance values between 10 and 30 nm.rad for the frame.

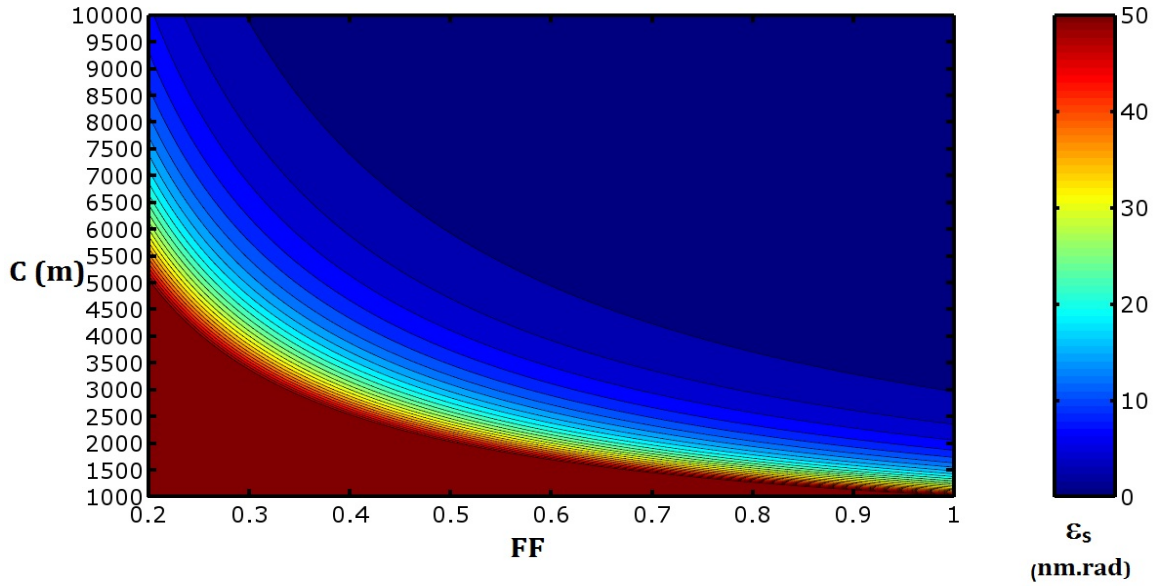


Fig. 5: Scaling of emittance with filling factor FF and circumference C for 20 GeV

3 Preliminary design

3.1 Assumptions and basic calculations

At the starting point of an accelerator design, there are important assumptions to be made and limitations to be determined, such as magnetic fields of magnets, energy loss per turn, and emittance. For this pre-booster design, the energy loss per turn is the main limitation. In the study, it is assumed that the energy loss per turn should be, at most, ≈ 50 MeV per turn, and the emittance can be taken to be 10 nm.rad. Some basic calculations show that this gives a dipole magnetic field of around 0.2–0.3 T with a total number N of about 260, and a bending angle of about 1.3° . Considering 140° for phase advance could be a good starting point. This gives us about 0.6–0.7 m^2 for the quadrupole strength. After all these assumptions and basic calculations, we find that our machine can be around 2.5 km long. Of course, these values will change after detailed calculations are made, as can be seen in the following part of this document. However, these calculations showed us that our studies were progressing in the right direction.

3.2 Chromaticity, phase advance and emittance

Chromaticity, phase advance and emittance: these three parameters are correlated with each other, as can be seen from Eqs. (3)–(7). Thus, in order to choose the optimized point for all three parameters, it is necessary to check how they change according to each other for a period of phase advance. For this, Figs. 6 and 7 are calculated from the relations [3–7].

$$\varepsilon_{\text{fodo}} = F_{\text{fodo}} C_q \gamma^3 \theta^3, \quad (3)$$

$$F_{\text{fodo}} = \frac{1 - \frac{3}{4} \sin^2(\phi/2)}{\sin^3(\phi/2) \cos(\phi/2)} J_x^{-1}, \quad (4)$$

$$\xi_{x0} = -\frac{1}{4\pi} \oint \beta_z k d_z, \quad (5)$$

$$\xi_{y0} = \frac{1}{4\pi} \oint \beta_y k d_z, \quad (6)$$

$$\phi = \arccos\left(\frac{1}{2} \text{trace}(M)\right). \quad (7)$$

The emittance (ε) depends on the lattice design factor (F) and the Lorentz factor (γ); C_q is 3.83×10^{-3} , θ is the total dipole bending angle in Eq. (3). F changes with phase advance (ϕ) as can be seen in Eq. (4), $J_x \approx 1$ is the damping partition number. Eqs. (5)–(6) shows the chromaticities in x and y directions. The chromaticity comes from the quadrupoles (k is the quadrupole strength) and it is proportional to the betatron function ($\beta_{z,y}$). Eq. (7) shows the dependency of the phase advance on the transfer matrix (M),

To see the relations between these parameters, Figs. 6–8 show ‘chromaticity–phase’, ‘chromaticity–emittance’, and ‘phase–emittance’ plots. All three of these plots are important but a study of the details of Fig. 8 could give us more information than the others in defining the optimum point.

Chromaticity increases with increasing phase advance for the period considered, as shown in Fig. 6.

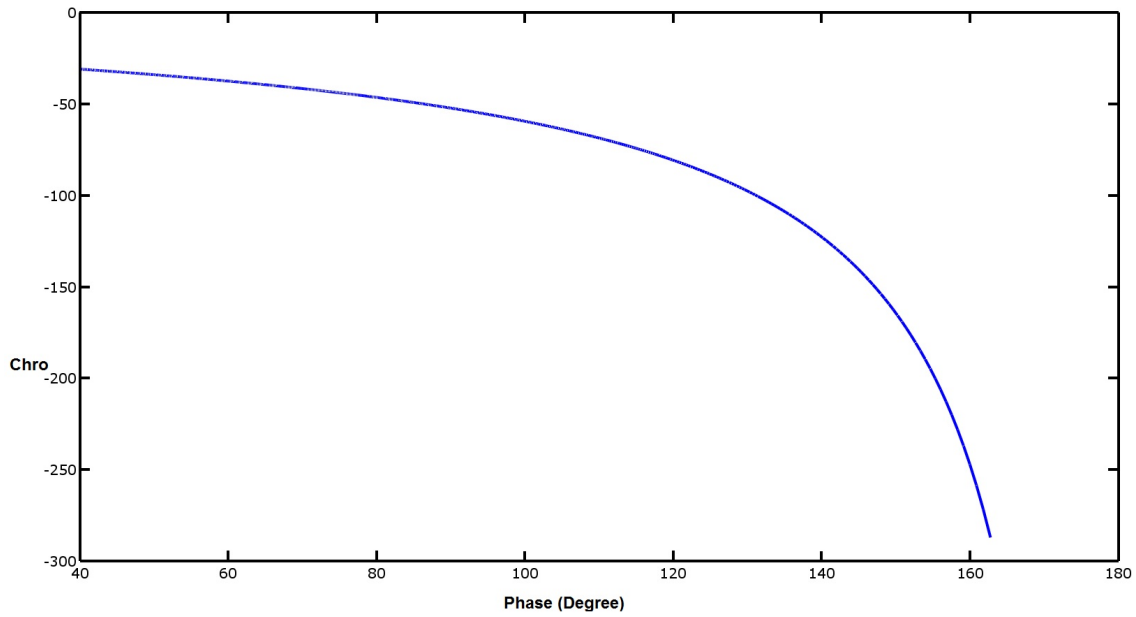


Fig. 6: Relation between chromaticity and phase

Figure 7 shows how emittance changes according to variations in phase advance.

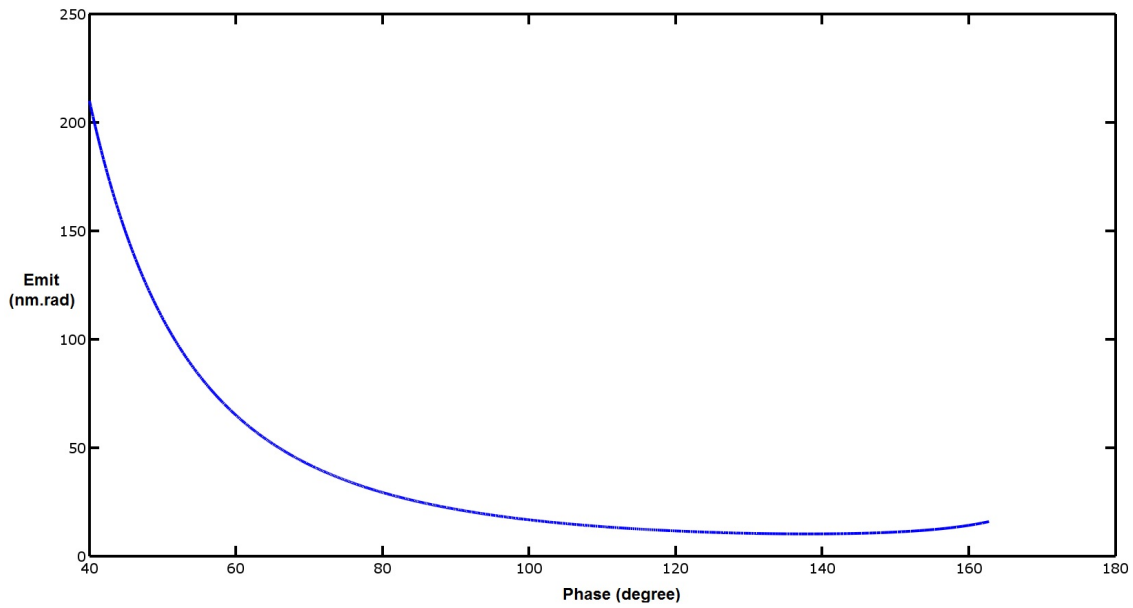


Fig. 7: Relation between emittance and phase advance

Figure 8 shows how emittance and chromaticity change with changes in phase advance. This graph also indicates that after some point the emittance does not vary so much, while the chromaticity changes very sharply. Therefore, this graph gives us useful information about choosing an optimized point for the machine.

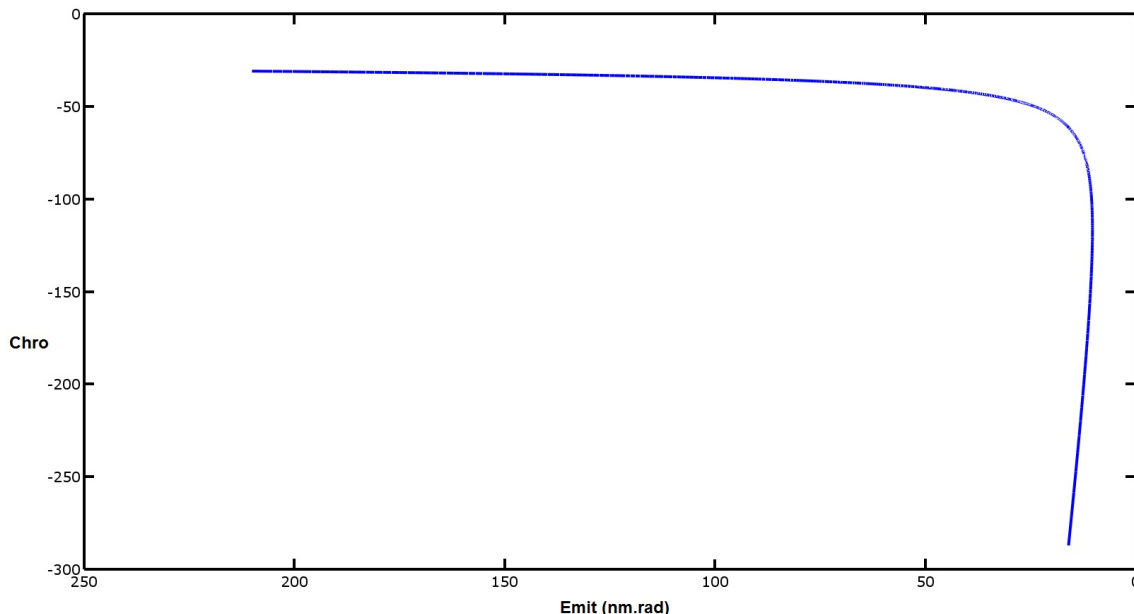


Fig. 8: Relation between chromaticity and emittance

3.3 Conceptual design

All results of abovementioned calculations and plots are evaluated, providing the most optimum design. A FODO type cell is chosen as the main cell for this ring. The ring comprises two arcs and two straight sections. In this design, the ring is 2321.95 m long and the corresponding FODO type cell is illustrated in Fig. 9.

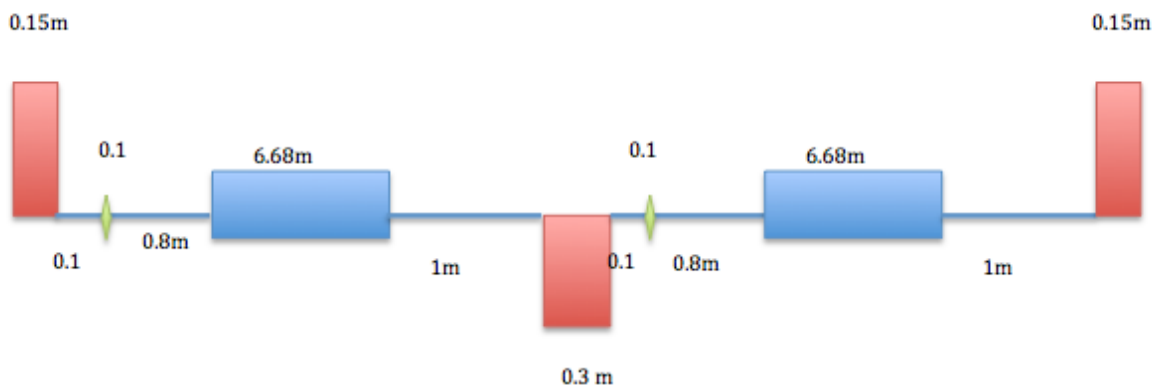


Fig. 9: Main cell of FODO, red shapes symbolize the focusing and defocusing quadrupole magnets, while blue represents bending magnets and green shows possible sextupole magnets.

Since natural chromaticities $\xi_x / \xi_y = -44.195/-42.358$ are high, it is also assumed to use sextupole magnets. In total, 260 dipole magnets (0.06 T/0.248 T) and 266 quadrupole and sextupole magnets are used in the ring. However, using sextupole magnets causes dynamic aperture problems. To limit the dynamic aperture effect, sextupole magnets with low strength are used in each cell instead of using only few sextupole magnets with high strength.

The beta function of the whole ring is shown in Fig. 10. For a booster ring, a straight section with zero dispersion must be allocated, because it is necessary for injection, extraction elements and for RF accelerating structures. From this figure, it can be seen that two straight sections are created in the design and the dispersion is decreased to zero with a matching cell in these sections.

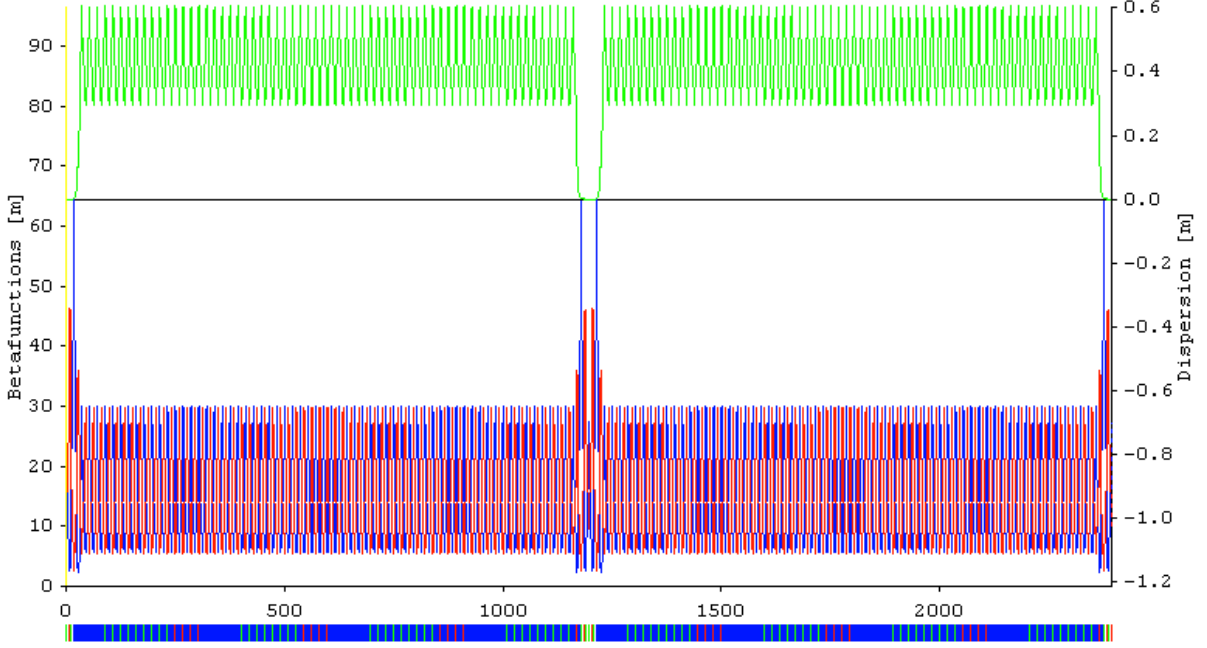


Fig. 10: Betatron functions of the whole ring; the maximum betatron functions (red and blue) around the ring is about 65 m and the dispersion (green) is zero in the straight sections.

The main parameters were calculated and are shown in Table 1.

Table 1: Main parameters

	Injection energy	Extraction energy
Energy	5.0 GeV	20 GeV
Perimeter	2393.54 m	2393.54 m
Emittance $\varepsilon_x/\varepsilon_y$	1.809 nm.rad	28.987 nm.rad
Energy spread (10^{-3})	0.258	1.034
Energy loss per turn	201.5 keV	51586.2 keV
Natural chromaticity ξ_x/ξ_y	-44.195/-42.358	-44.195/-42.358
Cell type	FODO	FODO

4 Conclusion

In this study, we have applied parameter scaling with respect to several radiation-related parameters and have proceeded with a preliminary design based on a FODO cell including sextupole magnets. The study presented in this document is a good starting point to see the general framework of the pre-booster by approaching it through analytical parameter scaling and studying the main parameters such as chromaticity, emittance and phase advance. In future studies, the calculations and preliminary design study will be compared with a study, which will use numeric approaches. It is expected that further studies like dynamic aperture, errors of momentum, alignment and multipolar will give additional limitations influencing the design of the pre-booster. Finally, by evaluating both analytic and numeric approaches, the design will converge further.

References

- [1] O. Etisken *et al.*, Preliminary design study of a pre-booster damping ring for the FCC e^-e^+ injector, FCC Week, Italy, 2016.
- [2] <https://home.cern/about/accelerators/super-proton-synchrotron>, last accessed 6 September 2016.
- [3] H. Wiedemann, *Particle Accelerator Physics* (Springer, Cham, 2007).
- [4] J. Rossbach *et al.*, Basic course on accelerator optics, CAS, 1993.S.Y. Lee, *Accelerator Physics*, 2nd ed. (World Scientific, Singapore, 2004). <https://doi.org/10.1142/5761>.